



HAL
open science

Ti-Doped Sapphire (Al₂O₃) Single Crystals Grown by the Kyropoulos Technique and Optical Characterizations.

Abdeldjelil Nehari, Alain Brenier, Gerard Panzer, Kheireddine Lebbou, Jerome Godfroy, Serge Labor, Herve Legal, Gilles Cheriaux, Jean-Paul Chambaret, Thierry Duffar, et al.

► **To cite this version:**

Abdeldjelil Nehari, Alain Brenier, Gerard Panzer, Kheireddine Lebbou, Jerome Godfroy, et al.. Ti-Doped Sapphire (Al₂O₃) Single Crystals Grown by the Kyropoulos Technique and Optical Characterizations.. *Crystal Growth & Design*, 2011, 11 (2), pp.445-448. 10.1021/cg101190q . hal-00633961

HAL Id: hal-00633961

<https://hal.science/hal-00633961>

Submitted on 30 Nov 2023

HAL is a multi-disciplinary open access archive for the deposit and dissemination of scientific research documents, whether they are published or not. The documents may come from teaching and research institutions in France or abroad, or from public or private research centers.

L'archive ouverte pluridisciplinaire **HAL**, est destinée au dépôt et à la diffusion de documents scientifiques de niveau recherche, publiés ou non, émanant des établissements d'enseignement et de recherche français ou étrangers, des laboratoires publics ou privés.

Ti-Doped Sapphire (Al_2O_3) Single Crystals Grown by the Kyropoulos Technique and Optical Characterizations

Abdeldjelil Nehari,[†] Alain Brenier,[†] Gerard Panzer,[†] Kheireddine Lebbou,^{*,†} Jerome Godfroy,[‡] Serge Labor,[‡] Herve Legal,[‡] Gilles Chériaux,[§] Jean Paul Chambaret, Thierry Duffar,[⊥] and Richard Moncorgé[#]

[†]Laboratoire de Physico-Chimie des Matériaux Luminescents (LPCML), UMR 5620, CNRS-Université de Lyon 1, 69622, Villeurbanne, France, [‡]RSA le rubis SA, BP 16, 38560 Jarrie/Grenoble, France, [§]LOA, ENSTA—Ecole Polytechnique, UMR 7639, Chemin de la Humière, 91761 Palaiseau Cedex, France, [⊥]ILE (Institut de Lumière Extrême), UMS 3205, Chemin de la Humière, 91761 Palaiseau Cedex, France, [⊥]SIMAP-EPM, BP75, Saint Martin d'Hères, 38402 Grenoble, France, and [#]CIMAP, UMR 6252, CEA-CNRS-ENSICAEN, Université de Caen, 14050 Caen, France

ABSTRACT: Transparent high optical quality and large Ti-sapphire (Ti^{3+} -doped Al_2O_3) single crystals have been grown by the Kyropoulos technique (KT) for optical amplification. The present work shows that by the utilization of KT growth technology and the optimization of the growth conditions it is possible to grow Ti-doped Al_2O_3 , 100 mm in diameter and 5 kg in weight. We have demonstrated that large Ti(0.25 atom %)-doped Al_2O_3 crystals show high chemical homogeneities and good optical properties and amplify the energy without any special annealing. Ti-doped sapphire crystals are for high power laser applications and particularly for the shortest pulses ever produced from a laser oscillator.

I. Introduction

Sapphire crystals are used for a wide range of applications: the clock and watch industry, synthetic jewelry, and optical components for microelectronics and laser systems. Today, there is an increasing demand for undoped sapphire wafers as substrates for GaN and ZnO thin films and for Ti^{3+} doped sapphire for ultrashort and high power laser systems. Sapphire doped with Ti^{3+} ions is now recognized as the solid state laser material which allows the direct generation of the shortest laser pulses and as the basic amplifier medium for most of the future high power laser chains at the petawatt level.^{1,2} Undoped and titanium-doped sapphire crystals are now considered as very strategic materials. Concerning the latter, a lot of work remains to be done to grow and provide high-quality large-size highly doped single crystals with reproducible performance. Improvements have been obtained here by working on the construction of the crystal growth equipment and by optimizing the growth process throughout different parameters. The numerical simulation and modeling of the equipment and processing have been an important tool for developing sapphire crystal growth in the industry.^{3–5} Today, the main sapphire growth techniques are the Verneuil, Czochralski, Stepanov, GOI (Musatov method), HEM (heat exchanger method), HDC (horizontal directional crystallization or Bagdasarov method), and Kyropoulos (KT) techniques. Although large undoped sapphire crystals have been grown by Khattak et al.⁶ by using the HEM technique and by Barish et al.⁷ by the temperature gradient technique (TGT), growth of large Ti^{3+} -doped Al_2O_3 crystals with a homogeneous titanium distribution and good optical quality is still a challenge. The main problem in Ti-sapphire crystal growth is strong segregation of the Ti^{3+} ions, because of their size difference with the substituted Al^{3+} ions, which generates

irremediable defects during the growth process. Moreover, the laser performance is often limited by optical loss infrared absorption bands of $\text{Ti}^{3+}-\text{Ti}^{4+}$ ion pairs⁸ that precisely occur in the laser emission wavelength. Annealing improves the quality of the as grown crystals. It allows changing partially Ti^{4+} into Ti^{3+} and improving the so-called figure of merit (FOM), which measures the ratio of the absorption coefficient at the pump wavelength of about 500 nm over the absorption coefficient associated with the parasitic $\text{Ti}^{3+}-\text{Ti}^{4+}$ absorption band around 800 nm. In the present paper, large size and highly Ti^{3+} -doped Al_2O_3 single crystals were successfully grown by the Kyropoulos technique (KT) at the RSA le Rubis Company and optical characterizations of the as grown crystals were performed.

II. Experimental Section

II-1. Starting Raw Materials. The starting raw materials were alumina and TiO_2 powders. The chemical components and the particle size of the starting raw materials were high purity TiO_2 (rutile) powders and undoped and Ti-doped α -alumina (Al_2O_3) of spherical micrometric geometry, in good agreement with JSPDS File No. 46-1212 ($a = 4.7570$ Å, $c = 12.9898$ Å), but traces of θ - Al_2O_3 (JSPDS File No. 86-1410) were also observed.

II-2. Crystal Growth. The Ti-sapphire crystals were grown by the Kyropoulos technique in a molybdenum (Mo) crucible with the diameter of the required crystal. Figure 1 shows a schematic illustration of the melt solidification inside the crucible. The crystal quality strongly depends on the hot zone of the Kyropoulos furnace. According to the thermal behavior during the growth process, this technique is considered within the framework of a 2D axisymmetric approach.⁹ The radiative heat exchange in the crystal and melt convection can be well controlled. Because of molybdenum crucible oxidation, high vacuum is necessary to avoid MoO_2 formation during the growth process. Two seed types were used, and the growth was initiated along the a - and c -axes. The total process including installation, heating up, the growth operation, and crystal cooling took about two weeks. Compared to the Czochralski and Bridgman techniques, this method uses a low thermal gradient in the

*Corresponding author: Kheireddine.lebbou@univ-lyon1.fr.

solidification region. The crystals do not cross a high gradient region above the crucible during the growth process, which is a good condition to eliminate the thermal stresses and to reduce the dislocation density.

III. Results

III-1. Grown Crystals. Figure 2 shows the grown crystals. The crystals were transparent and colored because of titanium doping. The diameter of the crystals was 100 mm, and their weight was about 5 kg, depending on the size of the crucibles and of the starting raw materials. Because of the sapphire high melting temperature (2050 °C) and the crystal size (diameter 100 mm), special care was taken to reduce the thermal losses from the crucible. The obtained crystals were exempt from macroscopic defects such as cracks, subgrain boundaries, and precipitates. For the laser applications, it is necessary to have the Ti^{3+} concentration in the crystals with the minimum level of Ti^{4+} and without titanium segregation. In order to reach the optimum titanium content, the crystals were grown from the melts with different Ti concentrations (0.15–0.35 atom %). According to our results, 0.25 atom % Ti in the melt was the good concentration to control the growth process (interface stability) and to obtain good quality transparent Ti-doped Al_2O_3 crystals under stationary stable conditions. At greater content of TiO_2 , the Al_2TiO_5 phase was formed. During the growth of large Ti-sapphire crystals by the Kyropoulos technique, high pulling rates and high rotation speeds induce vibrations and temperature variations of the crystallization interface, causing high thermal stresses. These factors decrease the optical quality of the crystals, and macroscopic defects such as bubbles and cracks, particular for large $Ti^{3+}-Al_2O_3$ crystals, were observed. The distribution of the Ti^{3+} ion along the crystals was inspected in different parts of the ingots by the ICP method. The unit cell volume increased in proportion to titanium concentration (Figure 3). Thus, the titanium concentration (X) can be estimated from the measurement of the unit

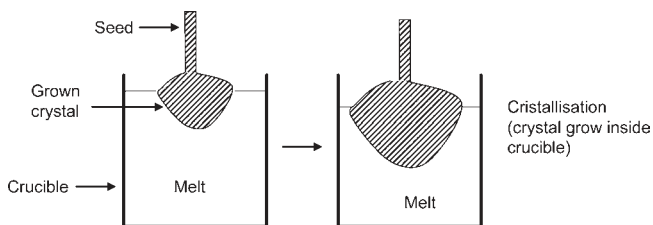


Figure 1. Schematic the Kyropoulos technique.



Figure 2. Sapphire ingots grown by the Kyropoulos technique: (a) *a*-axis; (b) *c*-axis; (c) wafer thickness 20 mm.

cell volume (\AA^3) using the approximation $V = 254.7141 + 0.8636[X]$. The segregation coefficient was calculated according to the Pfann¹⁰ equation, $C_s = kC_0(1 - g)^{k-1}$, where C_s is the Ti-dopant concentration in the crystal, C_0 is the starting dopant (Ti) concentration in the liquid, g is the melt solidification fraction and varies between 0 for the beginning of the growth and 1 when the entire melt was crystallized, and k is the segregation coefficient. The titanium segregation coefficient for the crystals grown by the Kyropoulos technique (this work) was measured to be 0.20. As was expected, due to the ionic radii difference between Ti^{3+} (60.5 pm) and Al^{3+} (53.3 pm), the segregation coefficient was small.

III-2. Optical Characterization. In order to estimate the intrinsic quality of the as grown Ti-sapphire crystals, we have used a nondestructive method based on the utilization of an He/Ne laser emitting at 633 nm.¹¹ A focused beam from the laser was sent through the crystal ($\phi = 100$ mm, $e = 15$ mm). The output intensity was recorded with a CCD digital camera connected to a computer. Whatever the growth direction (*a*-axis or *c*-axis), the best crystals were found exempt of defects, such as scattering, bubbles, and cracks, and demonstrated a near Gaussian profile of the transmitted laser beam (Figure 4), which is a first confirmation that the crystals were defect-free and of high optical grade. On the other hand, for higher titanium concentration, because of the presence of microscopic and macroscopic defects (bubbles, scattering), the beam profile of the grown crystals was non-Gaussian, with

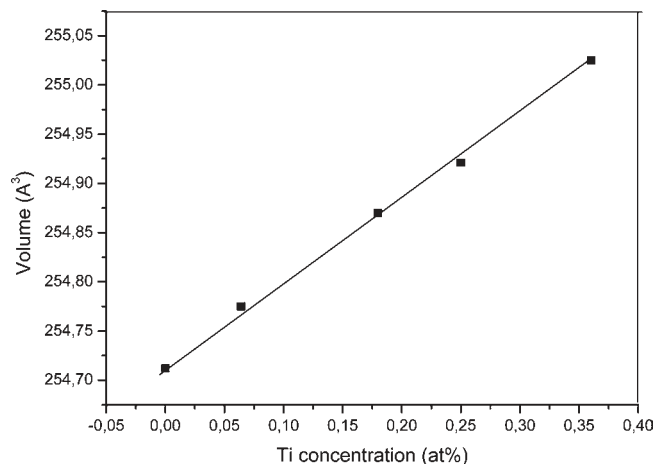


Figure 3. Evolution of volume as a function of titanium concentration in Ti-doped Al_2O_3 . Different fragments of the crystals were cut from the ingots and analyzed by X-ray diffraction and ICP.

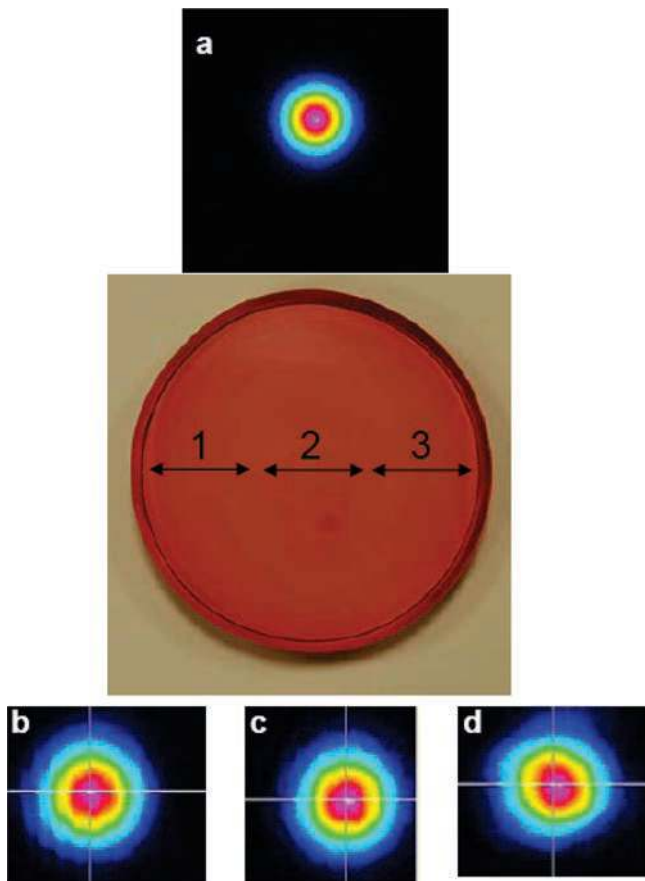


Figure 4. He/Ne laser beam shape ($P = 0.95$ mW) in air (a) and as passed through the crystal ($\phi = 100$ mm) in regions 1 (b), 2 (c), and 3 (d). The Ti starting concentration in the melt was 0.25 atom %.

a strong disturbance (Figure 5). The absorption spectra (Figure 6) of Ti^{3+} - Al_2O_3 at room temperature for different crystal orientations show two overlapping broad bands peaking around 490 and 525 nm, which correspond to two phonon side bands of the same Ti^{3+} optical transition from level 2T_2 to level 2E but split into two sublevels according to the Jahn–Teller effect.¹² In the α -sapphire lattice, Ti^{3+} ($3d^1$) substitutes Al^{3+} and is surrounded by an octahedron of oxygens with a slight trigonal distortion. The measured luminescence lifetime of Ti^{3+} (0.25 atom %) in Al_2O_3 was 3 μs at room temperature. A high concentration of Ti^{4+} ions could be responsible for some UV absorption, but this was not observed in our crystals. Moreover, crystals containing other impurities, such as iron (Fe), may show a broad absorption band and a long tail, extending well beyond 800 nm, and this band is usually related to a charge transfer transition between coupled iron–titanium ion pairs ($\text{Fe}^{3+}\text{Ti}^{3+} - \text{Fe}^{2+}\text{Ti}^{4+}$).¹³ A qualitative measurement of the Ti^{3+} spatial distribution inside the crystals was inspected by microluminescence analysis. The spectra were recorded on the crystals of 100 mm in diameter and 10 mm in thickness. For the measurement, the crystal was placed under a microscope (lens $\times 100$) and was directly excited with the focused beam of a 532 nm frequency-doubled and Q-switched Nd:YAG laser. The luminescence was recorded through the microscope by an optical fiber and transmitted to a monochromator that dispersed the emitted light onto a CCD detector cooled to 0 °C. The measurement was performed in different transversal sections of the crystal (Figure 7). The curves indicated higher luminescence intensity and higher Ti^{3+} ion concentration at the periphery of

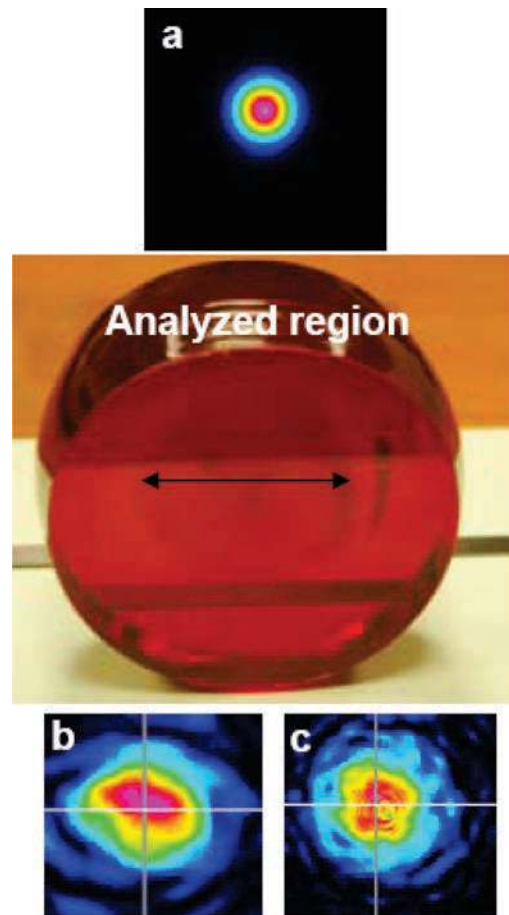


Figure 5. He/Ne laser beam shape ($P = 0.95$ mW) in air (a) and as passed through the crystal ($\phi = 100$ mm) regions (b, c) with defects.

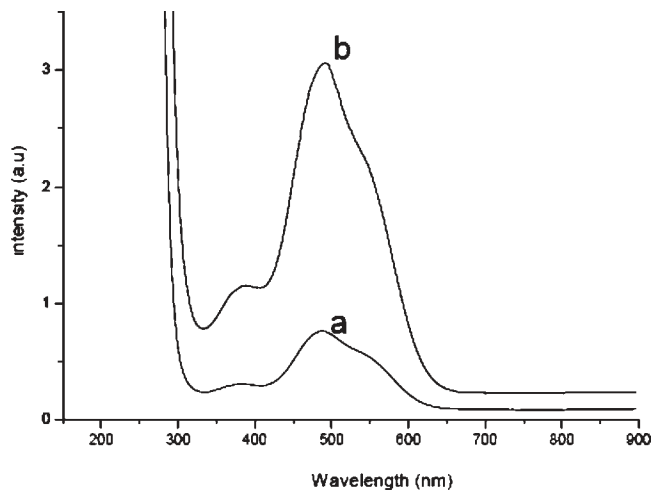


Figure 6. Room temperature absorption spectra of the as-grown Ti-sapphire single crystals grown by KT: (a) c -axis; (b) a -axis.

the crystal. The radial distribution of Ti^{3+} in the Ti-doped Al_2O_3 crystal expressed as luminescence at 730 nm is illustrated in Figure 8. There is a relatively large concentration gradient of Ti^{3+} at the periphery of the crystal, but the radial Ti distribution is rather homogeneous at the central part of the crystal. 80% of the crystal (80 mm) had homogeneous radial titanium concentration and allowed exploring a large part of the grown ingot. Following these results, it is possible to cut large laser rods or slabs along the plane perpendicular to the growth direction.

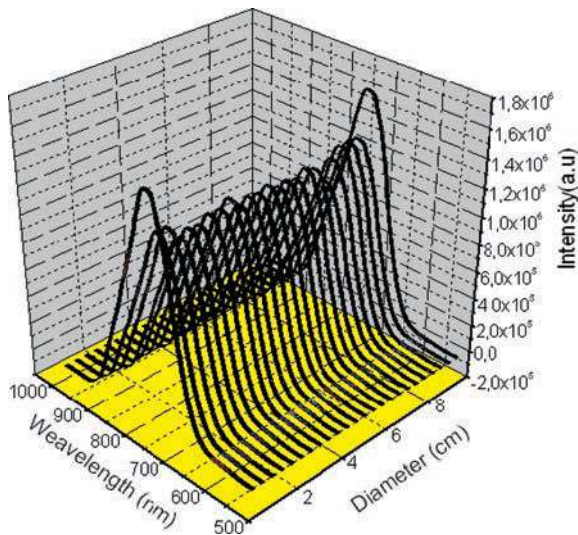


Figure 7. Microluminescence spectra (uncorrected for monochromator and detector response) recorded in different regions of the grown crystals (excitation of the Ti^{3+} luminescence at 532 nm).

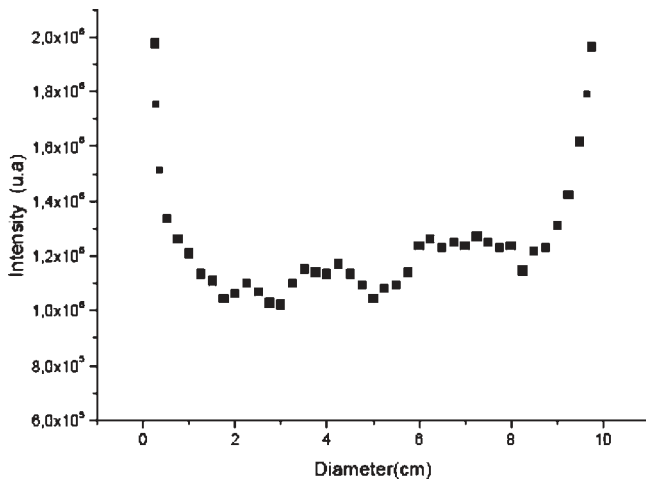


Figure 8. Profile of the Ti^{3+} ion distribution in the as grown Ti-sapphire crystal (starting titanium concentration in the melt was 0.25 atom %).

III-3. Optical Amplification. In order to validate the performance of the crystal, optical amplification experiment has been realized on a crystal of diameter 100 mm and thickness 50 mm. The crystal has been optically pumped by a frequency-doubled Nd:YAG laser, emitting 800 mJ of 532 nm light at a repetition rate of 10 Hz. The titanium doped sapphire crystal was positioned in a multipass amplifier (2 passes) of a classical chirped pulse amplification (CPA) laser chain. The seed pulses to be amplified have an energy of 8 mJ. An amplified energy of 65 mJ after the two passes has been obtained. The result is consistent with numerical calculations of amplification. In order to validate the spectroscopic characteristics of this crystal, we also measured the

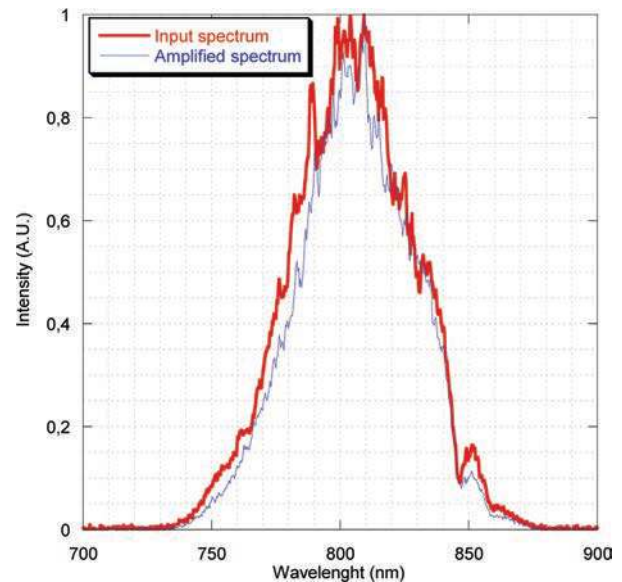


Figure 9. Input and amplified spectra of Ti-Al₂O₃ sapphire.

amplified spectrum and compared it to the input one. These two measurements are presented in Figure 9. This confirms that the doping of the sapphire host was completely adequate and in good agreement with the crystal quality.

IV. Conclusion

Large size and high optical quality (diameter 100 mm, weight 5 kg) Ti^{3+} -doped sapphire crystals have been successfully grown by the Kyropoulos technique. The crystals were transparent and exempt of cracks, inclusions, and other scattering centers. The crystals discussed in this work amplify the energy without any damaging. Without post growth annealing, the absorption and luminescence did not show the presence of unwanted impurities. The obtained results indicate homogeneous Ti^{3+} ion concentrations in large sections (80%).

References

- (1) Moulton, F. *J. Opt. Soc. Am.* **1986**, *B3*, 125–133.
- (2) Druon, F.; Balembois, F.; Georges, P. *C. R. Phys.* **2007**, *8*, 153–164.
- (3) Demina, S.-E.; Bystrova, E.-N.; Postolov, V.-S.; Eskov, E.-V.; Nikolenko, M.-V.; Marshinin, D.-A.; Yuferev, V.-S.; Kalaev, V.-V. *J. Cryst. Growth* **2008**, *310*, 1443.
- (4) Duffar, T.; Le Gal, H. *J. Cryst. Growth* **1999**, *198–199*, 239–245.
- (5) Theodore, F.; Duffar, T.; Louchet, F. *J. Cryst. Growth* **1999**, *198–199*, 232–238.
- (6) Khattak, C.-P.; Schmid, F. *J. Cryst. Growth* **2001**, *225*, 579.
- (7) Barish, B.-C. *IEEE Trans. Nucl. Sci.* **2002**, *49*, 1233–1236.
- (8) Sanchez, A.; Strauss, A.-J.; Aggarwal, R.-L.; Fahey, R.-E. *IEEE J. Quantum Electron.* **1988**, *24* (6), 995–998.
- (9) Demina, S.-E.; et al. *Opt. Mater.* **2007**, *30*, 62–65.
- (10) Pfann, W. *Zone melting*; John Wiley & Sons: New York, 1958.
- (11) Lebbou, K.; Perrodin, D. In *Advances in Materials Research*; Fukuda, T., Chani, V., Eds.; Springer-Verlag: 2007; pp 173–186.
- (12) Ham, F.-S. *Phys. Rev.* **1965**, *138*, 1727.
- (13) Powell, R.-C.; Caslavsky, J.-L.; Alshaieb, Z.; Bowen, J.-M. *J. Appl. Phys.* **1985**, *58* (6), 2331.